



PERGAMON

Journal of the Mechanics and Physics of Solids
50 (2002) 165–187

JOURNAL OF THE
MECHANICS AND
PHYSICS OF SOLIDS

www.elsevier.com/locate/jmps

Rate independent hysteresis in a bi-stable chain

G. Puglisi^a, L. Truskinovsky^{b,*}

^a*Dipartimento di Ingegneria Strutturale, Politecnico di Bari, Italy*

^b*Department of Aerospace Engineering and Mechanics, University of Minnesota, MN 55455, USA*

Received 2 January 2001; accepted 20 March 2001

The paper is dedicated to Professor Paolo Podio-Guidugli on the occasion of his 60th birthday

Abstract

The nontrivial behavior of an elastic chain with identical bi-stable elements may be considered prototypical for a large number of nonlinear processes in solids ranging from phase transitions to fracture. The energy landscape of such a chain is extremely wiggly which gives rise to multiple equilibrium configurations and results in a hysteretic evolution and a possibility of trapping. In the present paper, which extends our previous study of the static equilibria in this system (Puglisi and Truskinovsky, *J. Mech. Phys. Solids* (2000) 1), we analyze the behavior of a bi-stable chain in a soft device under quasi-static loading. We assume that the system is over-damped and explore the variety of available nonequilibrium transformation paths. In particular, we show that the “minimal barrier” strategy leads to the localization of the transformation in a single spring. Loaded periodically, our bi-stable chain exhibits finite hysteresis which depends on the height of the admissible barrier; the cold work/heat ratio in this model is a fixed constant, proportional to the Maxwell stress. Comparison of the computed inner and outer hysteresis loops with recent experiments on shape memory wires demonstrates good qualitative agreement. Finally we discuss a relation between the present model and the Preisach model which is a formal interpolation scheme for hysteresis, also founded on the idea of bi-stability. © 2002 Elsevier Science Ltd. All rights reserved.

Keywords: A. Phase transformation; Hysteresis; B. Elastic–plastic material; Lattice model; C. Energy methods; Cold work

1. Introduction

In today’s micro and nano-scale technologies the required complexity of the mechanical behavior can only be achieved if a “mechanism” is integrated into the material at

*Corresponding author. Tel.: +1-612-625-8000; fax: +1-612-626-1558.

E-mail address: trusk@aem.umn.edu (L. Truskinovsky).

the molecular level. “Active” or “intelligent” materials, exhibiting the desirable functions of sensing, actuation, damping, and feedback cannot be described by classical methods because of the genuinely nonlinear properties such as phase transformations, reversible pseudo-plasticity, and hysteresis. Another factor, which cannot be ignored at these extremely small sizes, is the presence of internal length scales, in particular, material discreteness. An interesting problem then is to start with a discrete model accounting for the nontrivial behavior of an active material at the micro-scale and develop comprehensive size-dependent quasi-continuum theory capable of describing its behavior at the technologically relevant meso-scales.

Martensitic phase transformations play a fundamental role in the behavior of a large class of active materials which include shape-memory, ferroelastic, and some magnetostrictive alloys (James and Hane, 2000; James and Wuttig, 1998). At the micro level, these materials can be viewed as complex assemblages of molecular size multi-stable devices; large deformations are then due to the switching between different locally stable configurations. Macroscopically the switching phenomena manifest themselves through the complicated evolution of the domain microstructures; the associated energy landscapes are usually extremely wiggly (Abeyaratne et al., 1996; Truskinovsky and Zanzotto, 1996; James, 1996; Ren and Truskinovsky, 2000).

The present paper is aimed at the analysis of rate independent hysteresis in shape memory alloys and other active materials through the study of the *simplest* representative discrete system with bi-stable elements. The discreteness of the system can be viewed as taking place at the level of the atomic lattice (crystal structure) or at some meso-scopic level, where it can be associated with the presence of defects, dislocations, polycrystalline grains, etc. The discrete approach to active materials can be traced back to the pioneering work of Müller and Villaggio (1977), who in the context of metal plasticity discretized a continuum model with nonconvex energy (Ericksen, 1975) and demonstrated numerically the existence of a multiplicity of additional, discretization-related equilibrium configurations. Since the model of Müller and Villaggio was motivated by an idea of actual mechanical snap-springs connected in series, the energy of an individual bi-stable element was chosen to be a rather complex trigonometric function. Subsequently Fedelich and Zanzotto (1992) by adopting a bi-parabolic approximation for the energy, were able to study the equilibrium configurations of the discrete system analytically and in more detail. More recently Puglisi and Truskinovsky (2000) clarified the issues of equilibrium and stability for the case of a general two well energy, particularly emphasizing the important role of the spinodal region. In the framework of the simplest bi-parabolic approximation, Rogers and Truskinovsky (1997) studied the role of an additional interaction ranging beyond the nearest-neighbors and provided a comparison of a non-local discrete model with the corresponding continuum model (see also Pagano and Paroni, 2000). The appearance of the artificial minima in the discretized versions of the non-convex variational problems in more than one dimension was discussed by Collins and Luskin (1994) and Kinderlehrer and Ma (1994). In the context of fracture mechanics, a discrete chain with non-convex springs of the Lennard–Jones type was considered in Truskinovsky (1996), Braides et al. (1999) and Del Piero and Truskinovsky (2000); a related model in biomechanics was investigated by Allinger et al. (1996).

An important open question, which lies outside the scope of these purely static analyses, concerns the actual strategies for the switching among the local minima inside the wiggly energy landscape. The most obvious strategy of following the global minimum (Maxwell path) was rejected early on because it is associated with the crossing of large barriers and does not lead to hysteresis (e.g. Müller and Villaggio, 1977). Another plausible strategy, based on the idea of thermal fluctuations and nonzero transition rates between the local minima, was suggested by Müller (1979) and studied in more detail in Müller and Wilmansky (1981), Achenbach and Müller (1985), Huo and Müller (1993), and Müller and Seelecke (1996). The model, which was shown to be in good agreement with some of the observations, predicts finite hysteresis whose width decreases with temperature. The main problem associated with this approach is the strict requirement it imposes on the value of the temperature, which cannot be too small. We also remark that this class of models excludes rate independent hysteresis in a quasi-static setting, which is the main subject of the present paper.

An alternative approach, which has also been explored, consists in modeling dynamics directly. The difficulty here is that even without external fluctuations, the full-scale inertial dynamics of the bi-stable chain is extremely complex. Thus, under a quasi-static loading the motion cannot be confined at long waves and intensive tunneling to short waves and high frequencies is taking place as the bi-stable units start to flip over from one configuration to another. The first dynamic solutions illustrating these phenomena for the simplest bi-linear chain were obtained by Slepyan and Troiankina (1984), who explicitly computed the kinetic relation for an isolated “switching” wave and gave a detailed description of the energy exchange between the macroscopic and the microscopic motions (see also Slepyan, 2000, 2001). More recently Balk et al. (2001a, 2001b), studied numerically the dynamical behavior of a finite bi-linear chain under cyclic loading, also emphasizing the importance of high frequency radiation and developing some thermodynamical interpretations. The relation between these purely mechanical approaches and the statistical approach of Müller and coauthors has yet to be established.

In the present paper in order to avoid a detailed description of the flip-over dynamics and the associated high frequency radiation, we assume that the system is overdamped, inferring that when an individual spring changes phase the excess energy completely dissipates into heat. We also assume that the presence of fluctuations allows the system to overcome energy barriers of a certain given size (see similar hypothesis in Fedelich and Zanzotto, 1992). With these two assumptions the evolutionary model is defined and we can characterize the non-equilibrium paths available to the system, in particular, the paths associated with crossing of the minimal energy barriers. As we show, this “minimal barrier” strategy leads to the localization of the transformation in a single spring, which may be a reason why the transformation often advances through the propagation of phase boundaries.

When loaded periodically, the bi-stable chain exhibits hysteresis whose width is inversely proportional to the square root of the size of the minimal barrier. In the case of low fluctuation activity, the system follows closely the maximum delay strategy and behaves very much like a conventional plastic system (modulo eventual saturation). In this limit one can develop a consistent thermodynamical theory and explicitly compute

the fraction of the work of the loading device dissipated into heat and the fraction stored in the chain in the form of a so-called “cold work”. Usually in thermo-plasticity the magnitude of the heat/cold work ratio is assumed to be constant (e.g. Rosakis et al., 2000). For our over-damped bi-stable chain with identical springs this ratio can be computed in closed form and can be shown to be in fact equal to a constant which depends on the Maxwell stress and the energy of the fluctuations.

The comparison of the fine structure of the predicted stress-strain relations with experiments shows that the model satisfactorily reproduces qualitative features of the hysteresis phenomena in shape memory wires and yields useful phenomenological description of the situations of interest to applications. In this respect the bi-stable chain can be compared to the Preisach model which is a standard mathematical tool for the phenomenological modeling of the rate independent hysteresis (e.g. Mayergoyz, 1991; Bertotti, 1999; Macki et al., 1993). As we argue, the two models are compatible; in particular our model reproduces important paradigms of the phenomenological Preisach model such as “return point memory” and “congruency”. The advantages of the bi-stable chain model are in the account of elasticity of the elements and in the ability of the system to choose between different metastable configurations.

The paper is organized as follows. In Section 2 we formulate the model and review some results concerning its equilibrium and stability. To illustrate the complexity of the energy landscape in Section 3 we consider in full detail an elementary example of a chain with two springs only. The general case is discussed in Section 4 where we show that the “minimal barrier” strategy leads to the localization of the transformation in one spring. In Section 5 we introduce some important thermodynamical concepts related to the hysteresis and compute the heat/cold work ratio. In Section 6 we discuss the mechanism of the transformation and study the inner structure of the hysteresis loops. Comparison with the phenomenological Preisach model is given in Section 6.1. The final section contains our main conclusions.

2. The model

In this section we introduce the model of bi-stable chain (Müller and Villaggio, 1977) and summarize its equilibrium and stability properties. For a more detailed analysis of these issues we refer the reader to Puglisi and Truskinovsky (2000).

Consider a one-dimensional lattice with N identical bi-stable elastic springs connected in series. Denote by u_i the displacements of the nodes and introduce the associated strains

$$\varepsilon_i = \frac{u_i - u_{i-1}}{a}, \quad (1.1)$$

where a is the reference length. If $a\varphi(\varepsilon_i)$ is the elastic energy of an individual spring, the free energy of the chain, normalized by its reference length, equals

$$\Phi = \frac{1}{N} \sum_{i=1}^N \varphi(\varepsilon_i). \quad (1.2)$$

We study the case when the springs are bi-stable, meaning that the elastic energy $\varphi(\varepsilon)$ is convex on two disjoint intervals (wells) separated by a region where it is concave (spinodal region); the corresponding stress–strain relation $\sigma = \varphi'(\varepsilon)$ is non-monotone. To simplify the analysis, we consider a special “tri-parabolic” energy

$$\varphi(\varepsilon) = \begin{cases} \frac{1}{2}(\varepsilon + 1)^2 + \sigma_M \varepsilon, & \varepsilon < -t, \\ \frac{1}{2}(\gamma \varepsilon^2 + \eta) + \sigma_M \varepsilon, & -t \leq \varepsilon \leq t, \\ \frac{1}{2}(\varepsilon - 1)^2 + \sigma_M \varepsilon, & t < \varepsilon, \end{cases} \quad (1.3)$$

which corresponds to a “tri-linear” stress–strain relation

$$\sigma(\varepsilon) = \begin{cases} \sigma_M + \varepsilon + 1, & \varepsilon < -t, \\ \sigma_M + \gamma \varepsilon, & -t \leq \varepsilon \leq t, \\ \sigma_M + \varepsilon - 1, & t < \varepsilon. \end{cases} \quad (1.4)$$

Here we assume that the equilibrium strains at $\bar{\sigma} = \sigma_M$ (Maxwell stress) are normalized to be ± 1 . To guarantee that the function φ is smooth we choose

$$\gamma = 1 - t^{-1}, \quad \eta = 1 - t, \quad (1.5)$$

where t is assumed to be in $(0, 1)$. One can show that this special choice of the energy function preserves all the qualitative features of the general bi-stable models (see Puglisi and Truskinovsky, 2000 for comparison).

Consider a chain with the energy (1.3) under the action of a prescribed stress $\bar{\sigma}$. To find equilibrium configurations of the individual springs we need to search for the minima of the total (potential) energy

$$G = \frac{1}{N} \sum_{i=1}^N \varphi(\varepsilon_i) - \bar{\sigma} \varepsilon_i. \quad (1.6)$$

The equilibrium equations take the form

$$\varphi'(\varepsilon_i) = \bar{\sigma}, \quad i = 1, \dots, N. \quad (1.7)$$

For a given stress $\bar{\sigma}$, Eq. (1.7) may have up to three solutions corresponding to the three branches of the nonmonotone stress–strain relation. In what follows we distinguish these solutions by indexes I, II and III (see Fig. 1). More specifically, we obtain

$$\varepsilon_{\text{I}} = \tilde{\sigma} - 1, \quad \varepsilon_{\text{II}} = \frac{\tilde{\sigma}}{\gamma}, \quad \varepsilon_{\text{III}} = \tilde{\sigma} + 1, \quad (1.8)$$

where

$$\tilde{\sigma} := \bar{\sigma} - \sigma_M. \quad (1.9)$$

Due to the uniformity of the spring stiffnesses and to the absence of long range interactions, the total energy $G(\varepsilon_1, \dots, \varepsilon_N)$ is invariant under the permutations of its arguments. As a consequence the equilibrium solutions (1.8) at fixed $\bar{\sigma}$ may be grouped

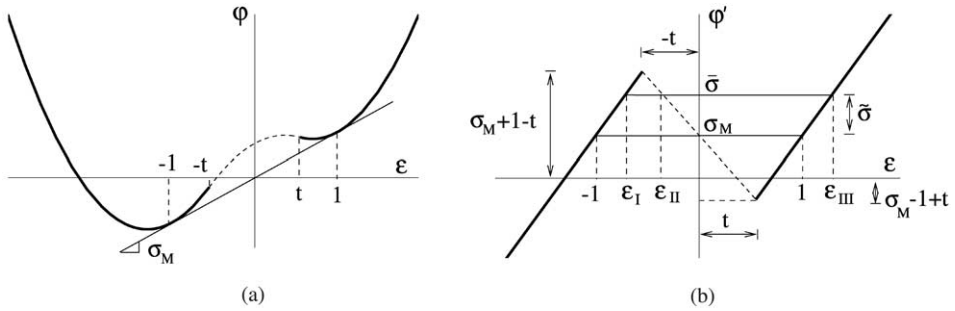


Fig. 1. Elastic energy (a) and stress–strain relation (b) for the “tri-linear” model. Here $t = 0.5$ and $\sigma_M = 0.2$.

into iso-energetic equivalence classes. Each class can be identified by the phase fractions (k, l, m) indicating the number of springs in phases I, II, and III, respectively; obviously $k + l + m = N$. For given phase fractions the overall strain

$$\bar{\varepsilon} = \frac{1}{N} \sum_{i=1}^N \varepsilon_i \tag{1.10}$$

can be computed explicitly as a function of the applied stress. The resulting stress–strain relation is linear.

$$\bar{\varepsilon}(\bar{\sigma}) = \frac{\bar{\sigma}}{E} + \varepsilon_0 \tag{1.11}$$

with

$$E = \frac{N\eta}{N\eta - l}, \tag{1.12}$$

representing the effective elastic modulus and

$$\varepsilon_0 = \frac{m - k}{N}, \tag{1.13}$$

representing the “eigenstrain” at $\bar{\sigma} = \sigma_M$. The multivalued stress–strain relation (1.11) is illustrated in Fig. 2(a).

According to Eqs. (1.6) and (1.8) the total energy of equilibrium solutions can be written in the form

$$G(\bar{\sigma}) = -\frac{\bar{\sigma}^2}{2E} - \bar{\sigma}\bar{\varepsilon}_0 + \frac{1}{2} \frac{l}{N} \eta. \tag{1.14}$$

This expression is illustrated in Fig. 2(b), where we see the characteristic cusps associated with the nonsingle-valuedness of the Legendre transform in Eq. (1.6). The total elastic energy of the chain (1.2) can be written as

$$\Phi(\bar{\sigma}) = \frac{\bar{\sigma}^2}{2E} + \frac{1}{2} \frac{l}{N} \eta + \sigma_M \bar{\varepsilon}(\bar{\sigma}). \tag{1.15}$$

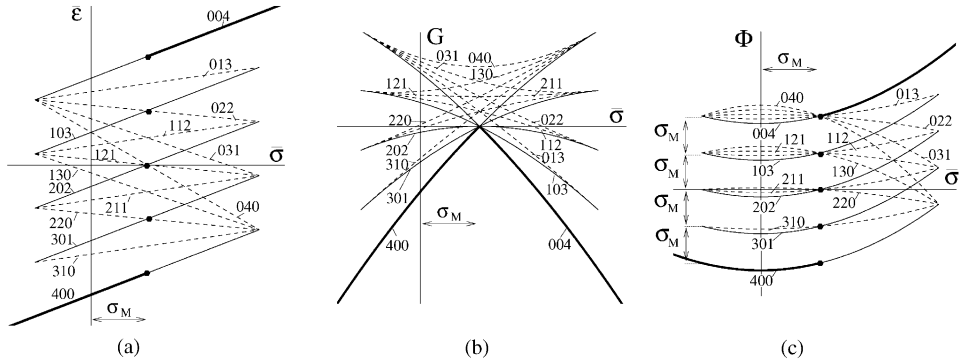


Fig. 2. Overall stress–strain relation: (a) potential energy, (b) and elastic energy, (c) for a chain with four springs, $N = 4$. The branches are distinguished by the corresponding phase fractions (k, l, m) . Local minima are represented by solid lines, unstable equilibrium configurations by dashed lines, and global minima by bold lines. Here $t = 0.6$, $\sigma_M = 0.2$.

The stress dependence of the elastic energy (1.15) is illustrated in Fig. 2(c). One can show that the branches corresponding to the same number l of springs in the spinodal region collapse to a single parabola in the limit $\sigma_M = 0$.

The trajectories corresponding to the global minimum of the potential energy are indicated in Fig. 2 by the bold lines. We remark that along the global minimum path all snap-springs change phase at the Maxwell stress: the system then overcomes a set of barriers jumping into new equilibrium configurations with the same total, but higher elastic energies. Notice that during these transitions the chain stores all the work done by the loading device.

Local stability of the above equilibrium solutions was analyzed in Puglisi and Truskinovsky (2000). In particular, it was found that an equilibrium configuration is metastable (is a local minimum of the potential energy) if and only if none of the strains takes values inside the spinodal region. This means that in metastable configurations necessarily $l = 0$ and that the only observable branches of equilibria are the ones with phase fractions $(k, 0, N - k)$. The stability of different branches is illustrated in Fig. 2 where stable solutions are indicated by bold lines, metastable by solid lines, and unstable by dashed lines.

Analysis of Fig. 2 suggests that several metastable configurations may correspond to a given value of the loading parameter. As a result, different scenarios of quasi-static evolution are possible depending on the system ability to overcome energy barriers. To make this point more clear, in the next section we discuss a simple example illustrating the complexity of the full energy landscape and the multiplicity of the possible evolution strategies.

3. Elementary example

For the purpose of making our general considerations in the subsequent sections more transparent, we begin with a study of a chain with two springs only, $N = 2$. Also, to

make figures less cluttered we assume in this section that $\sigma_M = 0$ which amounts to removing a linear term from the energy and does not effect the main conclusions. Maxwell stress will be restored in Section 5.

Instead of dealing with the individual strains ε_1 and ε_2 it is convenient to introduce order parameters $\bar{\varepsilon}$ and $\bar{\zeta}$ according to

$$\varepsilon_1 = \bar{\varepsilon} - \bar{\zeta}, \quad \varepsilon_2 = \bar{\varepsilon} + \bar{\zeta}. \quad (2.1)$$

Here the first order parameter $\bar{\varepsilon}$ is the overall strain; the second order parameter $\bar{\zeta}$ measures the deviation from the symmetric state $\varepsilon_1 = \bar{\varepsilon}$, $\varepsilon_2 = \bar{\varepsilon}$. In terms of the order parameters the total energy can now be written as

$$\hat{G} = \frac{1}{2}(\varphi(\bar{\varepsilon} + \bar{\zeta}) + \varphi(\bar{\varepsilon} - \bar{\zeta})) - \bar{\sigma}\bar{\varepsilon}. \quad (2.2)$$

The fact that configurational space is two dimensional makes it possible to study in detail the energy landscape for different values of the external load $\bar{\sigma}$. With our tri-parabolic expression for the energy φ it is straightforward to compute $\hat{G}(\bar{\varepsilon}, \bar{\zeta})$; our results are summarized in Fig. 3.

We observe that if $\bar{\sigma} \in (t-1, 1-t)$ energy (2.2) exhibits three different local minima m_1, m_2, m_3 corresponding to the metastable branches $(2, 0, 0)$, $(1, 0, 1)$, and $(0, 0, 2)$, respectively. The global minimum of the energy is at $(2, 0, 0)$ for $\bar{\sigma} < 0$ and at $(0, 0, 2)$ for $\bar{\sigma} > 0$.

The knowledge of the energy landscape allows one to study the nonequilibrium paths connecting local and global minima. Suppose for determinacy that $\bar{\sigma} = \bar{\sigma}_3 \in (0, 1-t)$ as represented in Fig. 3(e) and consider the metastable configuration $m_1(2, 0, 0)$. One can see that the path from this local minimum, characterized by the minimal energy barrier, goes through the saddle configuration $s_1(1, 1, 0)$ with one spring stable and another one in the spinodal region. In the configurational space the local minimum $m_1(2, 0, 0)$ is connected to the two symmetric saddles $s_1(1, 1, 0)$ and further to the symmetric inhomogeneous local minima $m_2(1, 0, 1)$ by the straight lines

$$\bar{\zeta} = \pm \bar{\varepsilon} \pm (1 - \bar{\sigma}). \quad (2.3)$$

To illustrate the physical meaning of trajectories (2.3), consider first one of the paths: $\bar{\zeta} = -\bar{\varepsilon} - (1 - \bar{\sigma})$. Along this path $\varepsilon_2 = \bar{\sigma} - 1$ which means $\varphi'(\varepsilon_2) = \bar{\sigma}$ so that the spring $i=2$ is in equilibrium. The other spring $i=1$ is not equilibrated ($\varphi'(\varepsilon_1) \neq \bar{\sigma}$) and instead changes phase. Analogously, along the path $\bar{\zeta} = \bar{\varepsilon} + 1 - \bar{\sigma}$ we observe that $\varphi'(\varepsilon_1) = \bar{\sigma}$ and $\varphi'(\varepsilon_2) \neq \bar{\sigma}$ so that now the spring $i=2$ changes phase. Once the system reaches the saddles s_1 , the trajectories (2.3) are the paths of steepest descent to the minima m_2 (paths of maximum rate of dissipation). Notice also that from the critical state s_1 both minima m_2 of $(1, 0, 1)$ and m_3 of $(0, 0, 2)$ may be reached without overcoming other energy barriers; however out of the two, only the minimum m_2 can be reached by the path of steepest descent.

Similar analysis can be done for the “minimal barrier” trajectories leading away from the metastable states m_2 . The corresponding saddles (s_2) and the minimum (m_3) are connected in the configurational space by the straight lines

$$\bar{\zeta} = \pm \bar{\varepsilon} \mp (1 + \bar{\sigma}), \quad (2.4)$$

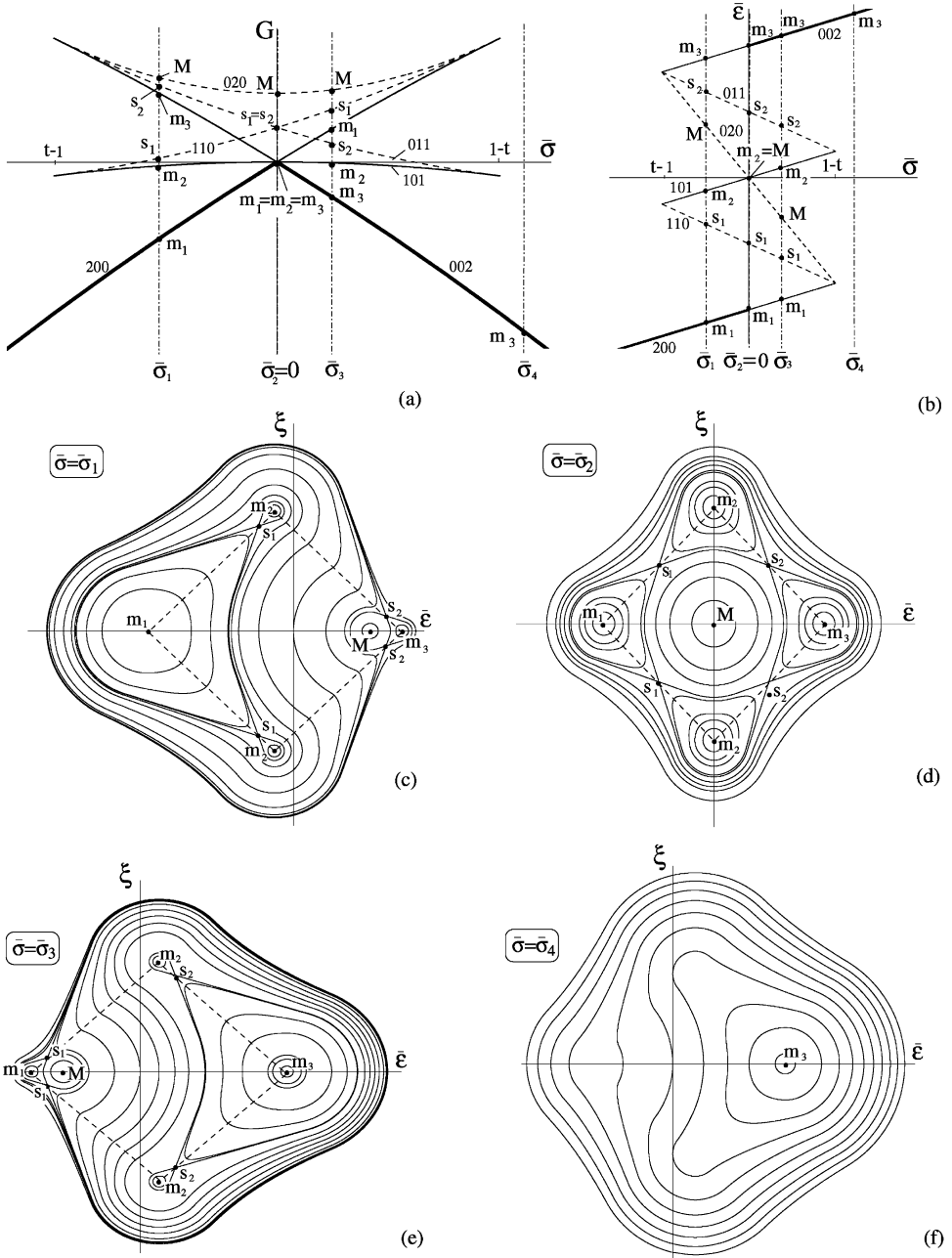


Fig. 3. Energy landscape for the chain with $N=2$ shown at different values of $\bar{\sigma}$. In (c), (d), (e), and (f) the energy levels are represented by solid lines; dashed lines correspond to “minimal barrier” paths. The barriers are also illustrated in Fig. 4. Here $t=0.8$ and $\sigma_M=0$.

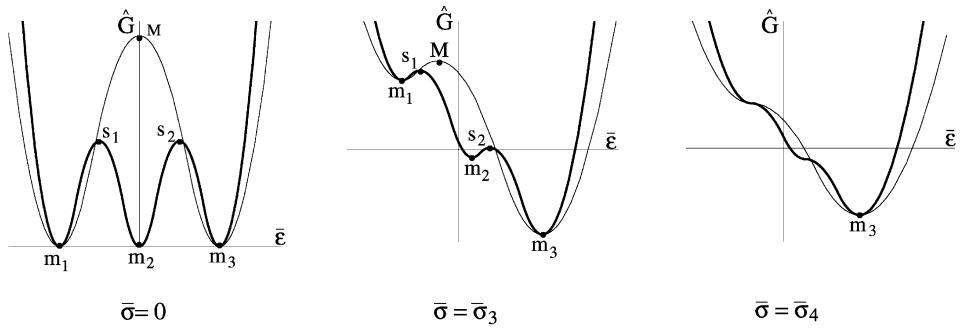


Fig. 4. Free energy along the “minimal barrier” paths (2.3) and (2.4) (bold lines) and along the “Cauchy–Born” path $\zeta = 0$ (solid line). The stress values are chosen in accordance with Fig. 3.

describing again the paths with one spring in equilibrium and another one changing phase.

By considering the two transitions $m_1 \rightarrow s_1 \rightarrow m_2$ and $m_2 \rightarrow s_2 \rightarrow m_3$ together we can make the important observation that along the “minimum barrier” paths the phase transition proceeds as a sequence of events with one spring changing phase at a time and the other spring fixed. In the next section we show that this behavior is generic at any N .

Further insights are provided by Fig. 4 where we illustrate the energy variation along our “minimal barrier” paths (2.3), (2.4) which we compare with the homogeneous “Cauchy–Born” path $\zeta = 0$. One can see that a sequential change of phase by the individual springs is preferred over simultaneous transition of the whole chain. Notice that in this figure only the essential part of the energy landscape is shown with all irrelevant degrees of freedom minimized out. In the next sections we shall be using similar synthetic representation of the energy landscape adjusted to the case of a general N .

4. General case

The analysis of the special case in Section 3 suggests the conjecture that the “minimal barrier” path can always be represented as a combination of the successive switching events inside the individual springs with all other springs equilibrated. In this section we prove this conjecture; to make the analysis more transparent we shall keep the assumption $\sigma_M = 0$.

First, we recall that at a given N the global minimum of the energy is located at the trivial branches of equilibria: $(N, 0, 0)$ if $\bar{\sigma} < 0$, $(0, 0, N)$ if $\bar{\sigma} > 0$; the only metastable configurations are the two-phase states $(k, 0, N - k)$. We assume that $\bar{\sigma} > 0$ and choose a particular metastable configuration

$$\hat{\epsilon}_i = \begin{cases} \bar{\sigma} - 1, & i = 1, \dots, \hat{k}, \\ \bar{\sigma} + 1, & i = \hat{k} + 1, \dots, N. \end{cases} \tag{3.5}$$

To prove the conjecture we need to show that the “minimal barrier” path leading away from this metastable state goes necessarily through the saddle¹ configuration $(\hat{k} - 1, 1, N - \hat{k})$ with one of the \hat{k} springs in the spinodal state $\varepsilon = \varepsilon_{\text{II}}$.

We begin with the construction in the space of strains $\{\varepsilon_i\}$ of a cube \mathcal{C} with center in our metastable configuration (3.5): $|\varepsilon_i - \hat{\varepsilon}_i| \leq r$. The side of the cube $r = \varepsilon_{\text{II}} - \varepsilon_{\text{I}}$ is chosen in such a way that the saddle $S(\hat{k} - 1, 1, N - \hat{k})$ belongs to the boundary of the cube $\partial\mathcal{C}$. Since for $\bar{\sigma} > 0$

$$|\varepsilon_{\text{I}} - \varepsilon_{\text{III}}| > |\varepsilon_{\text{II}} - \varepsilon_{\text{III}}| > |\varepsilon_{\text{I}} - \varepsilon_{\text{II}}| = r, \quad (3.6)$$

the only critical point in the interior of the cube \mathcal{C} is given by Eq. (3.5). Therefore, we need to show that the minimum energy on $\partial\mathcal{C}$ is given by the saddle S .

Consider one of the planes belonging to $\partial\mathcal{C}$, say $\varepsilon_j = e_j$ with $e_j = \hat{\varepsilon}_j \pm r$. Minimization of the energy function $G(\varepsilon_1, \dots, \varepsilon_N) = \sum_{i=1}^N \varphi(\varepsilon_i) - \bar{\sigma}\varepsilon_i$ on this plane gives the following necessary conditions:

$$\varphi'(\varepsilon_i) = \bar{\sigma}, \quad i = 1, \dots, j-1, j+1, \dots, N. \quad (3.7)$$

Let us denote with $\{\tilde{\varepsilon}_i\}_{i=1, \dots, N}$ the generic solution of Eq. (3.7) with $\tilde{\varepsilon}_j = e_j$; this solution belongs to $\partial\mathcal{C}$, if

$$\begin{aligned} \tilde{\varepsilon}_i &\in \{\varepsilon_{\text{I}}, \varepsilon_{\text{II}}\}, \quad i \in \{1, \dots, \hat{k}\}, \quad i \neq j, \\ \tilde{\varepsilon}_i &= \varepsilon_{\text{III}}, \quad i \in \{\hat{k} + 1, \dots, N\}, \quad i \neq j. \end{aligned} \quad (3.8)$$

Introduce the Gibbs free energy of the single spring $g(\varepsilon) = \varphi(\varepsilon) - \bar{\sigma}\varepsilon$. Since

$$h = g(\varepsilon_{\text{II}}) - g(\varepsilon_{\text{I}}) = \frac{(\bar{\sigma} + t - 1)^2}{2(1-t)} \geq 0 \quad (3.9)$$

and

$$G(\varepsilon_i) = \sum_{i=1}^N g(\varepsilon_i) \quad (3.10)$$

the critical point (3.8) with the minimal energy necessarily satisfies

$$\tilde{\varepsilon}_i = \hat{\varepsilon}_i, \quad i \neq j. \quad (3.11)$$

Now, we need to minimize the energy of the critical points among the different planes $\varepsilon_j = e_j$. If $j \in \{1, \dots, \hat{k}\}$ and $e_j = \varepsilon_{\text{I}} + r$, which corresponds to the saddle $S(\hat{k} - 1, 1, \hat{m})$, we obtain

$$G(\tilde{\varepsilon}_i) = G(\hat{\varepsilon}_i) + h. \quad (3.12)$$

If instead $e_j = \varepsilon_{\text{I}} - r$, then

$$G(\tilde{\varepsilon}_i) = G(\hat{\varepsilon}_i) + h + \frac{t(\bar{\sigma} + t - 1)^2}{2(1-t)^2} \geq G(\hat{\varepsilon}_i) + h. \quad (3.13)$$

¹ According to the “mountain pass theorem” (e.g. Struwe, 1990) the minimum barrier out of the basin necessarily corresponds to a saddle point.

If on the other hand $j > \hat{k}$ and $e_j = \varepsilon_{\text{III}} + r$, then

$$G(\tilde{\varepsilon}_i) = G(\hat{\varepsilon}_i) + h + \frac{t(\bar{\sigma} + t - 1)^2}{2(1-t)^2} \geq G(\hat{\varepsilon}_i) + h. \quad (3.14)$$

Finally, if $j > \hat{k}$ and $e_j = \varepsilon_{\text{III}} - r$ we have two possibilities. For $\varepsilon_{\text{III}} - r > t$, e_j is in the second well and the energy is again given by Eq. (3.14). If, on the contrary, the j th spring is in the spinodal region, i.e. $\varepsilon_{\text{III}} - r < t$ which according to Eq. (1.8) means

$$\bar{\sigma} < \frac{t(1-t)}{2-t}, \quad (3.15)$$

we obtain

$$G(\tilde{\varepsilon}_i) = G(\hat{\varepsilon}_i) + h + \frac{2\bar{\sigma}(-\bar{\sigma} + t(1-t))}{t(1-t)} \geq G(\hat{\varepsilon}_i) + h. \quad (3.16)$$

By comparing the energies of these critical points we conclude that the ones with the lowest energy are the saddles $S(\hat{k} - 1, 1, \hat{m})$.

Similar analysis can be made for the $(N - l)$ dimensional planes belonging to $\partial\mathcal{C}$ with l constrained springs; one can again show that the critical points with lowest energy are the ones with all the non constrained strains taking values $\tilde{\varepsilon}_i = \hat{\varepsilon}_i$. Indeed, when all the l constrained strains take the values ε_{II} we obtain

$$G(\tilde{\varepsilon}_i) = G(\hat{\varepsilon}_i) + lh > G(\hat{\varepsilon}_i) + h. \quad (3.17)$$

One can check that even bigger energies are obtained in the other relevant cases which completes the proof of our conjecture.

Once the system possesses sufficient activation energy to exit the basin of the metastable configuration (3.5), it can reach any of the \hat{k} local minima with $\hat{k} - 1$ springs in the first well. By using the invariance properties of the energy one can always assume that it is the \hat{k} th spring which changes phase. As in the case $N = 2$, we can consider a trajectory which passes through one of the above saddles with one spring changing phase and all the other springs staying in equilibrium with the load. This corresponds to the minimization of the energy with respect to all ε_i with $i \neq \hat{k}$. We can again choose the total strain $\bar{\varepsilon}$ as the order parameter and write

$$\varepsilon_i(\bar{\varepsilon}) = \begin{cases} \bar{\sigma} - 1, & i = 1, \dots, \hat{k} - 1, \\ \varepsilon_{\hat{k}}(\bar{\varepsilon}), & i = \hat{k}, \\ \bar{\sigma} + 1, & i = \hat{k} + 1, \dots, N, \end{cases} \quad (3.18)$$

where

$$\varepsilon_{\hat{k}}(\bar{\varepsilon}) = N\bar{\varepsilon} - (\hat{k} - 1)(\bar{\sigma} - 1) - \hat{m}(\bar{\sigma} + 1). \quad (3.19)$$

The trajectory (3.18) describes the transition $(\hat{k}, 0, \hat{m}) \rightarrow (\hat{k} - 1, 1, \hat{m}) \rightarrow (\hat{k} - 1, 0, \hat{m} + 1)$ and presents an exact generalization of the paths (2.3) and (2.4). It is not hard to show that this path corresponds to the steepest descent (and maximum rate of dissipation) from the saddle point $(\hat{k} - 1, 1, \hat{m})$ to the minimum $(\hat{k} - 1, 0, \hat{m} + 1)$. Indeed, along the trajectory (3.18) for $i \neq \hat{k}$ we have $d\varepsilon_i(\bar{\varepsilon})/d\bar{\varepsilon} = 0$ and $dG/d\varepsilon_i = \varphi'(\varepsilon_i(\bar{\varepsilon})) - \bar{\sigma} = 0$, which means that the two vectors are parallel.

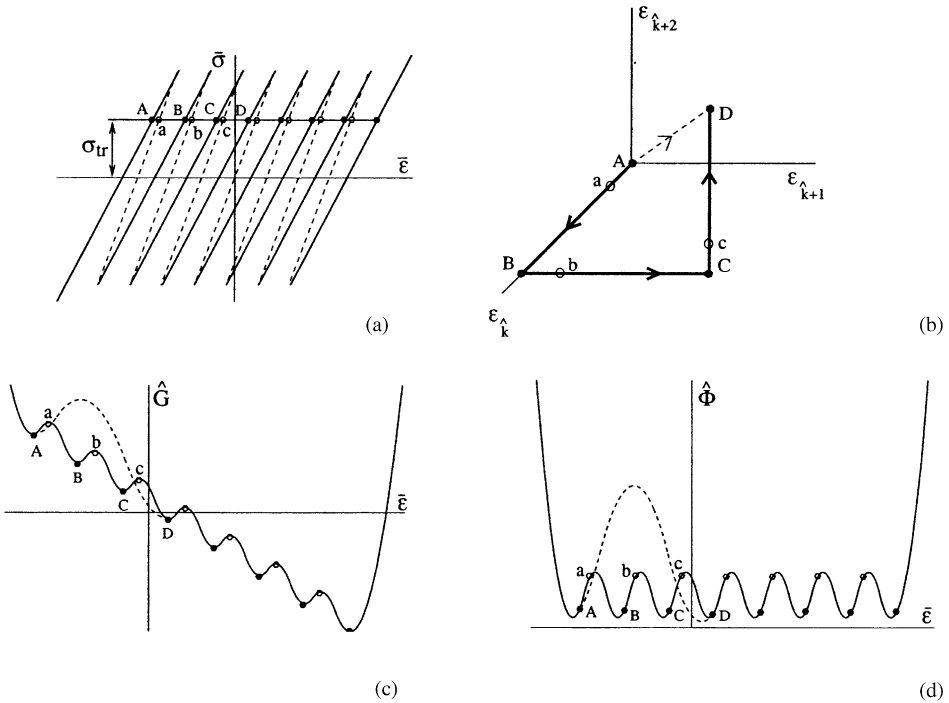


Fig. 5. Non-equilibrium total and elastic energies along three successive minimum barrier paths (3.18). Capital letters indicate metastable states, lowercase letters are saddle points. The paths are represented in the stress–strain space (a), and in the $\{\varepsilon_i\}$ space (b). In (b)–(d) the paths (3.18) are compared with a partial “Cauchy–Born” path (three springs changing phase simultaneously, dashed line). Here $\sigma_M = 0$, $t = 0.5$, $\sigma_{tr} = 0.3$.

A complete transition between the branches $(N, 0, 0)$ and $(0, 0, N)$ can now be obtained as a combination of N different paths of the type (3.18). The composition of three successive steps in the space $\{\varepsilon_i\}$ is illustrated in Fig. 5 where the “minimal barrier” path (ABCD) is compared with the path describing all three springs changing phase simultaneously (AD); one can see that along the direct path AD the system encounters a much higher barrier.

Notice that along the minimal barrier path each individual jump delivers a strain increment

$$[\bar{\varepsilon}] = \frac{2}{N}, \tag{3.20}$$

which is independent of the phase fractions (of \hat{k}). The variation of the total energy of the chain along this path can be computed directly from

$$\hat{G}(\bar{\varepsilon}) = \frac{1}{N}((\hat{k} - 1)\varphi(\bar{\sigma} - 1) + (N - \hat{k})\varphi(\bar{\sigma} + 1) + \varphi(\varepsilon_{\hat{k}}(\bar{\varepsilon}))) - \bar{\sigma}\bar{\varepsilon}. \tag{3.21}$$

In particular, one can verify that $d\hat{G}_{\hat{k}}(\bar{\varepsilon})/d\bar{\varepsilon} = \varphi'(\varepsilon_{\hat{k}}(\bar{\varepsilon})) - \bar{\sigma} > 0$ as we ascend from the local minimum $(\hat{k}, 0, N - \hat{k})$ to the saddle $(\hat{k} - 1, 1, N - \hat{k})$ and that $d\hat{G}_{\hat{k}}(\bar{\varepsilon})/d\bar{\varepsilon} < 0$ as we descend from the saddle to another local minimum $(\hat{k} - 1, 0, N - \hat{k} + 1)$. The associated energy barrier is equal to

$$h(\bar{\sigma}) = \frac{1}{2} \frac{(\bar{\sigma} + t - 1)^2}{N(1 - t)}. \quad (3.22)$$

One can see that the height of the barrier (3.22) is a decreasing function of $\bar{\sigma}$. At the Maxwell stress we get the maximum barrier

$$h_m = \frac{1}{2} \frac{1 - t}{N}, \quad (3.23)$$

while at the spinodal stress we obtain $h = 0$. If the system possesses an activation energy $h_a < h_m$, then the transition stress may be obtained by the inversion of Eq. (3.22)

$$\sigma_{tr} = (1 - t) - \sqrt{2Nh_a(1 - t)}. \quad (3.24)$$

To proceed with our analysis we need to make an important assumption that when the load reaches the value σ_{tr} and one spring changes phase the released energy completely dissipates into heat. The magnitude of the dissipated energy is equal to

$$Q = -\frac{2\sigma_{tr}}{N}. \quad (3.25)$$

Since at $\sigma_M = 0$ the elastic energy increment associated with this discontinuous transition is equal to zero, the dissipated energy exactly matches the work of the loading device; this conclusion will be modified in the next section where we consider the case $\sigma_M \neq 0$. After a full hysteresis cycle of loading and unloading the elastic energy remains unchanged while the total dissipation is finite and equals to

$$Q_{\text{cycle}} = 2NQ = -4\sigma_{tr}. \quad (3.26)$$

The largest dissipation corresponds to the maximum delay convention with $h_a = 0$. Then $\sigma_{tr} = 1 - t$ and $Q_{\text{cycle}} = -4(1 - t)$.

5. Cold working

Consider now the case of a general N and $\sigma_M \neq 0$; the main consequence of the latter modification is that now the local minima corresponding to the same stress have different elastic energies.

Most of the results from the previous section are still valid with a replacement of $\bar{\sigma}$ by $\tilde{\sigma} := \bar{\sigma} - \sigma_M$. Thus the lowest energy barrier is now

$$\tilde{h}(\tilde{\sigma}) = \frac{1}{2} \frac{(\tilde{\sigma} + t - 1)^2}{N(1 - t)}, \quad (4.27)$$

where again the maximum value corresponds to the Maxwell stress $\bar{\sigma} = \sigma_M$ and the zero barrier to the spinodal stress $\bar{\sigma} = \sigma_M + 1 - t$. For a given activation energy h_a

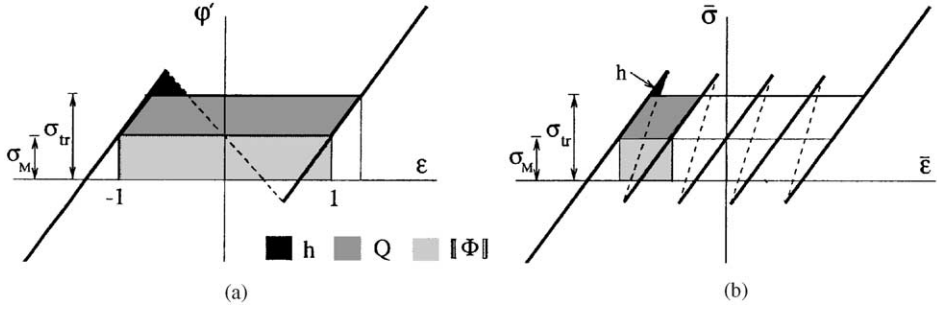


Fig. 6. The dissipated energy Q and the cold work $[\Phi]$ in the cases $N = 1$ (a) and (b).

we may again define the corresponding transformation stresses

$$\sigma_{tr}^{\pm} = \sigma_M \pm (1 - t - \sqrt{2Nh_a(1-t)}). \quad (4.28)$$

The dissipated energy associated with one jump $[\bar{\varepsilon}] = 2N^{-1}$ is now

$$Q = -(\sigma_{tr}^+ - \sigma_M)[\bar{\varepsilon}] = -\frac{2(\sigma_{tr}^+ - \sigma_M)}{N}. \quad (4.29)$$

The energy dissipated in a full cycle is then

$$Q_{\text{cycle}} = -4(\sigma_{tr}^+ - \sigma_M). \quad (4.30)$$

For systems with $\sigma_M \neq 0$ (see the schemes of Figs. 6 and 7) the elastic energy is not constant during the transitions inside the individual springs and instead experiences incremental jumps equal to

$$[\Phi] = \sigma_M[\bar{\varepsilon}] = \frac{2\sigma_M}{N}. \quad (4.31)$$

Along each of the nonequilibrium paths the work $W = \sigma_{tr}^+[\bar{\varepsilon}]$ of the external load can now be decomposed into a part Q which is dissipated and a part $[\Phi]$ which is elastically stored by the system (*cold work*). Usually in plasticity cold work is associated with accumulation of defects or dislocations; in our model each switching to a well with higher energy may also be interpreted as a structural defect. One can then calculate the fraction of the work done by the loading device which dissipates into heat over the work stored in the system. Since $W = \sigma_{tr}^+[\bar{\varepsilon}] = 2\sigma_{tr}^+/N$, we obtain

$$\beta = -\frac{Q}{W} = \frac{\sigma_{tr}^+ - \sigma_M}{\sigma_{tr}^+}. \quad (4.32)$$

As we see this ratio is constant. We recall that the assumptions concerning the constancy of the heat/cold work ratio are at the core of most phenomenological formulations of thermoplasticity (e.g. Rosakis et al., 2000).

Consider now the reverse path when the load $\bar{\sigma}$ is decreasing. In this case the system changes phase at $\bar{\sigma} = \sigma_{tr}^-$ with $[\bar{\varepsilon}] = -2N^{-1}$ and $Q = (\sigma_M - \sigma_{tr}^-)[\bar{\varepsilon}] = 2(\sigma_{tr}^- - \sigma_M)/N$, which, according to Eq. (4.28), is exactly the same value as we obtained in Eq. (4.29). In this case $[\Phi] = \sigma_M[\bar{\varepsilon}] = -2\sigma_M/N$ which means that the cold work produced in the

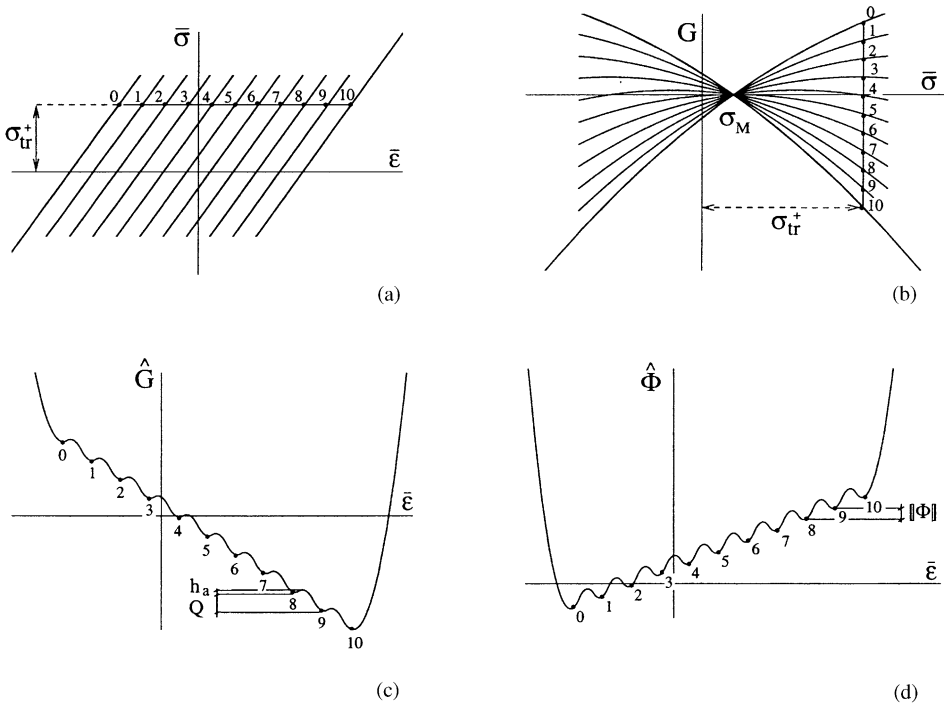


Fig. 7. Equilibrium and nonequilibrium energies in the case of nonzero Maxwell stress, $\sigma_M \neq 0$, $N = 10$.

direct transition is completely returned in the reverse transition. The fact that the cold work can be recovered in a cyclic process makes transformational plasticity a reversible (albeit nonequilibrium) process.

The representative graphs for the equilibrium and nonequilibrium free and potential energies are shown in Fig. 7.

6. Transformation mechanism and hysteresis

We begin the analysis of the transformation mechanism in the present model with a discussion of the suitability of our “minimal barrier” strategy which we compare with the conventional criteria based on the consideration of the driving forces. We recall that our activation energy criterion asserts that the system continues to be in a local minimum until the smallest energy barrier around this state reaches below a fixed threshold. Then the system leaves its metastable configuration and jumps into the closest local minimum which can be achieved through the steepest descent path originating in the corresponding saddle point. This last process is considered to be dissipative and along the way the system is treated as overdamped (gradient flow); the activation energy is returned to the system while the rest of the released energy dissipates into heat.

The driving force criterion is based on the assumption that in the two well system with fluctuations, probabilities of transitions in both directions have to be considered. As a result, the overall transformation rate depends on the relative depth of the wells which in our case is the dissipated energy. The driving (or configurational) force f can then be defined as the dissipated energy normalized by the advance of the transformation. For instance, in the case of simultaneous switch of p springs we obtain

$$f := - \frac{Q(p)}{p[\bar{\varepsilon}]} = \sigma_{tr}^+ - \sigma_M. \quad (5.1)$$

Notice that f does not depend on the number p of transforming springs and, as a result, the critical driving force criterion does not select the transition path with one single spring changing phase at a time.

It is not hard to see, however, that the two criteria discussed above are not completely independent. Indeed, the height of the minimal barrier h and the driving force f are related through

$$h = \frac{(f + t - 1)^2}{2N(1 - t)}. \quad (5.2)$$

One can see that the driving force grows with stress, while the energy barrier decreases with it; however, fixed barrier trajectories are also characterized by fixed driving force. As a result, both criteria (critical barrier size and critical driving force) lead to the transformation taking place at a *constant* stress.

The actual mechanism of the transformation can be viewed in the following form. According to both criteria, once the transformation is activated, it propagates with a particular speed which depends on how fast the system can actually dissipate the released energy. In the “minimal barrier” scenario the chain absorbs the activation energy h provided from outside and releases the excess energy: the activation part of the excess energy is returned to the system, while the driving force part is dissipated. Since at fixed stress the energy barriers are also fixed, the activation energy, released in crossing one barrier, can be used to excite another transition. The process can then repeat itself resulting in a self-sustained, autocatalytic propagation of the switching wave. We recall that the individual jumps are highly localized with only one spring being “out of equilibrium” at a given transition. The process of phase transition can thus be viewed as a propagation of a front rather than gradual transformation inside an extended area. It is clear that in our simplified model the interaction between the springs is too weak to actually favor interface migration over successive formation of new interfaces in random places; this however can be fixed if the interaction of next to nearest neighbors is taken into consideration (e.g. Rogers and Truskinovsky, 1997). Different phenomenological models of the phase boundary migration, compatible with the above scheme, have been recently reviewed in Ngan and Truskinovsky (1999).

The knowledge of the energy landscape allows one to describe the whole loading process starting from $\tilde{\sigma} < t - 1$ when the only minimum of the energy is $(N, 0, 0)$. When $t - 1 < \tilde{\sigma} < 0$ multiple metastable configurations other than the homogeneous state $(N, 0, 0)$ are available to the system, although the corresponding driving force is negative and the barriers are high. When the load reaches the Maxwell level the

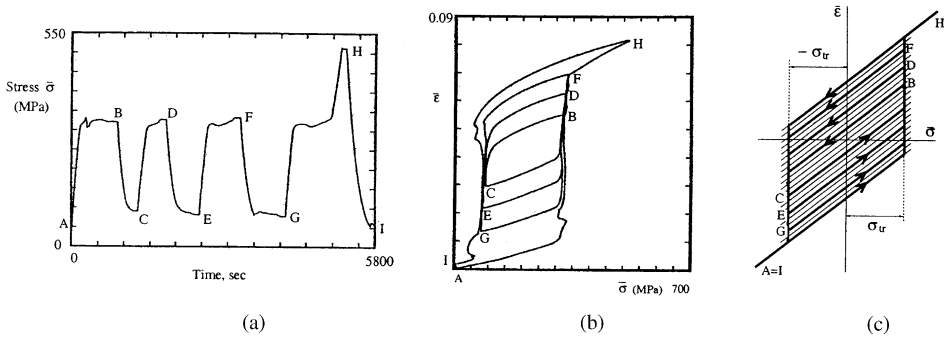


Fig. 8. Experimental behavior of a Ni–Ti shape memory wire in a soft device under cyclic loading (courtesy of T. Shield) compared with the hysteretic behavior of a bi-stable chain.

system discovers alternative inhomogeneous configurations with the same energy as the original homogeneous state. In this case the driving force is zero; however, the barriers may still be high. In the interval $0 < \bar{\sigma} < 1 - t$ the transformation will necessarily start at some critical stress $\bar{\sigma} = \sigma_{tr}$ which is controlled either by the condition that the driving force is sufficiently large or by an equivalent condition that the barriers are sufficiently small. Then the system dynamically evolves towards configurations characterized by lower total energy, switching along the way one spring at a time.

Now, consider the cyclic loading test which can be compared with the recent experiments on Ni–Ti shape memory wires reported in Maher et al. (1999). The typical experimental data are shown in Fig. 8. As we see, the hysteresis loops may be decomposed into the upper stress plateau corresponding to the transition between the cubic (austenite) and the monoclinic (martensite) phases, the lower stress plateau corresponding to the reverse transition, and the two connecting edges where the system behaves elastically. Notice that both internal and external loops are characterized by (almost) the same magnitude of the phase transition stresses σ_{tr} . The above properties can be reproduced by our discrete model if we assume that the activation energy is selected in such a way that the direct transformation takes place at $\bar{\sigma} = \sigma_{tr}$ while the reverse transformation occurs at $\bar{\sigma} = -\sigma_{tr}$. If the load is kept fixed at $\pm\sigma_{tr}$ a complete transition takes place which corresponds to the “outer hysteresis loop” shown in Fig. 8(c). “Internal loops” may be observed if the load is reverted before the transition is complete. As in the experiment, the loops may be decomposed into the plateaux where “plastic” deformation takes place, joined by the edges with purely “elastic” deformation. Since the edges are located inside the hysteresis area this observation leads to the apparently “paradoxical” conclusion that all deformations inside the hysteresis are elastic.

Finally we remark that our analysis refers to the quasistatic loading programs only, when the (nonlinearity driven) energy transfer to high frequencies can be considered instantaneous at the time scale of the loading. Other effects associated with a finite speed of heat removal and supply are observed experimentally at higher rates of loading (e.g. Leo et al., 1993; Shaw and Kiriakides, 1995; Shield et al., 1997) and require more sophisticated modeling.

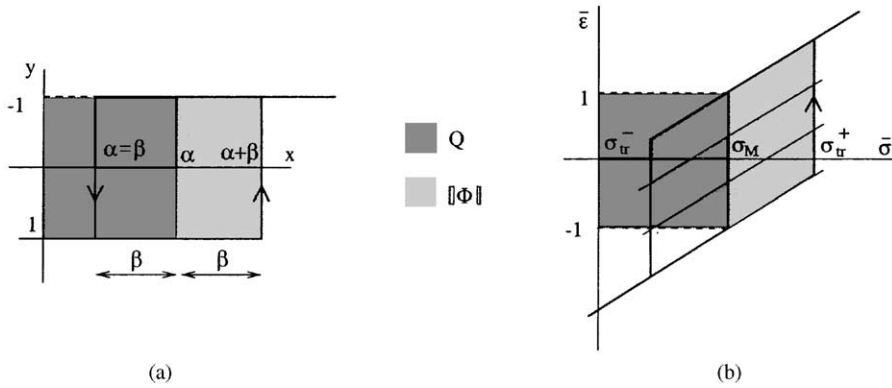


Fig. 9. Classical Preisach element and “elastic” Preisach element describing the behavior of the tri-linear snap-spring.

6.1. Preisach model

In this section we compare our model with the classical Preisach model which is widely used in the description of hysteresis in both mechanical and magnetic systems (Bertotti, 2000; Ortin, 1992).

According to the Preisach model, any hysteretic system which satisfies certain definitive properties (see, for instance, Mayergoyz, 1991) can be *formally* represented as a collection (or as a continuous distribution) of noninteracting bi-stable elements. Each element can occupy two configurations which are described by an output parameter y taking values ± 1 . The precise value of y depends on the value of the input parameter x through a hysteretic constitutive operator shown in Fig. 9(a); the hysteresis loop of a sample element is characterized by two parameters α and β whose values are distributed with a probability density $p(\alpha, \beta)$. The average output can be calculated from the formula

$$\bar{y}(\bar{x}) = \int_{\mathcal{R}_+} p(\alpha, \beta) d\alpha d\beta - \int_{\mathcal{R}_-} p(\alpha, \beta) d\alpha d\beta, \tag{5.3}$$

where \mathcal{R}_+ is the region in the (α, β) plane where $y = 1$, while \mathcal{R}_- is the complementary region; by knowing the evolution of these domains one can keep track of the loading history.

The similarity between the Preisach model and our chain with bi-stable elements loaded in a soft device is quite obvious. First, the input parameter x of the Preisach model is an exact analog of our applied stress; in the absence of the interaction beyond nearest neighbors, the applied stress acts in our case as a mean field. The role of the output parameter y is played in our model by the strain ϵ_i . The stress–strain relation for our individual bi-stable element is hysteretic: the two parameters of the Preisach element α and β can be identified in the present case with the Maxwell stress σ_M and the transformation stress $\tilde{\sigma}_{tr} := \sigma_{tr}^+ - \sigma_M$. One can also relate the gray area in Fig. 9(a) for the Preisach element with our cold work and the black area on the same graph with our dissipation (see Fig. 9(b)).

In spite of these apparent similarities, the two models are quite different; in particular the overall response in the mechanical model is potentially much richer than in the Preisach model. This may not be so transparent in the present treatment because, due to the uniformity of the bi-stable elements, the resulting Preisach distribution is trivial (reduces to a delta function).

To highlight the differences between the models we notice that the spring lengths in our model are not constrained to take specific values and exhibit elastic response; in this sense a Preisach element can be viewed as a limit of our snap-spring unit with an infinite elastic modulus. The most important difference, however, is that in our model the nonequilibrium configurations of the individual elements are not controlled directly by the applied stress. As a result our model generates additional possibilities for the system of being trapped in the local minima separated by the corresponding energy barriers which gives rise to a much broader class of evolution strategies ranging from no hysteresis at all to the paths with a maximal delay.

The simplest way to compare the models is to look at the special case of the Preisach model when all elements are identical. In this case the classical Preisach model predicts that all elements transform at once which eliminates the possibility of the inner loops observed in the experiment (see Fig. 8). On the contrary, our model with identical elements is compatible with locking in a variety of metastable configurations.

The simplest adaptation of the Preisach model to our case can be obtained if one adds an elastic term in Eq. (5.3) and assumes that the parameters of the two models are chosen to be compatible. Specifically, since all the elements are identical, we define

$$p = p(\alpha, \beta) = \delta(\alpha - \sigma_M) \delta(\beta - (\sigma_{tr}^+ - \sigma_M)), \quad (5.4)$$

where σ_M characterizes the elementary contribution to cold work $[\Phi] = 2\sigma_M$, while $\sigma_{tr}^+ - \sigma_M$ gives a measure of the associated dissipation $Q = -2(\sigma_{tr}^+ - \sigma_M)$.

Due to the elasticity of the elements we have to modify the standard Preisach formula for the average output by adding a purely elastic term. We obtain

$$\begin{aligned} \bar{\varepsilon}(\bar{\sigma}(t)) = & \bar{\sigma} - \sigma_M + \int_{\mathcal{R}^+} \delta(\alpha - \sigma_M) \delta(\beta - (\sigma_{tr}^+ - \sigma_M)) d\alpha d\beta \\ & - \int_{\mathcal{R}^-} \delta(\alpha - \sigma_M) \delta(\beta - (\sigma_{tr}^+ - \sigma_M)) d\alpha d\beta. \end{aligned} \quad (5.5)$$

To illustrate this formula, consider a case when the stress is increasing beginning from the homogeneous configuration with $(\sigma_M, \sigma_{tr}^+ - \sigma_M) \in \mathcal{R}^-$. Then according to Eq. (5.5) $\bar{\varepsilon}(\bar{\sigma}) = \bar{\sigma} - \sigma_M - 1$ and the model chooses the homogeneous branch $(N, 0, 0)$. At $\bar{\sigma} = \sigma_{tr}^+$ all elements change phase. Now, $(\sigma_M, \sigma_{tr}^+ - \sigma_M) \in \mathcal{R}^+$ which corresponds to the other homogeneous branch $(0, 0, N)$ with all the elements in the second well and $\bar{\varepsilon}(\bar{\sigma}) = \bar{\sigma} - \sigma_M + 1$. If the load continues to increase the system stays, according to Eq. (5.5), on the same branch. If now the load is decreased, the elements change phase again at $\bar{\sigma} = \sigma_{tr}^-$ and the system evolves according to the condition that $(\sigma_M, \sigma_{tr}^+ - \sigma_M) \in \mathcal{R}^-$. As a result the system completes the same loop as our bi-stable discrete system (see Fig. 8(c)), exhibiting the return point memory and congruency properties (see Mayergoyz, 1991). Based on this analysis we can conclude that once elasticity is introduced, the modified Preisach model shows the same outer loops as our

discrete system. At the same time, the inner loops shown in Fig. 8, originating from the possibility for our discrete system to be trapped in each of the metastable states, cannot be reproduced by the modified Preisach model. We should mention, however, that the failure of the present version of the Preisach model to generate a richer class of internal loops should be partially attributed to the degeneracy of the special Preisach distribution considered here; essentially in this version of the Preisach model we are dealing with one bi-stable element.

7. Conclusions

In this paper we studied the simplest prototypical mechanical system exhibiting some of the most important features of shape memory alloys and some other active materials: microstructure formation, propagation of phase boundaries, large reversible deformations, and hysteresis. The main characteristics of the model responsible for these constitutive properties are *discreteness* and the *nonconvexity* of the elemental energy. A careful study of the interplay between discreteness and nonconvexity is crucial for the understanding of rate independent hysteresis and other phenomena associated with the trapping of the material in the wiggly energy landscape.

Specifically, we considered a cyclic loading in a soft device of an overdamped discrete chain with N bi-stable snap-springs. For simplicity of computations the energy of an individual snap-spring was chosen to be tri-parabolic, which partially linearized the problem. This simplification allowed us to study in detail the complicated energy landscape of this system at arbitrary N and quantify nonequilibrium paths associated with the minimal energy barriers. As we showed, in a complete loading–unloading cycle our overdamped elastic chain behaves like an elastoplastic element. The cycle contains $2N$ quantized advances of the transformation; each of these advances is externally activated and is accompanied with a finite dissipation. Due to the analytical simplicity of the model we could also evaluate at each step of the loading program the fraction of the energy irreversibly transformed into heat.

According to our model, the hysteresis loops may be decomposed into two stress plateaux reflecting the transition processes and a multiplicity of connecting edges where no phase transition is taking place. Characteristically, both internal and external loops are distinguished by the same magnitude of the transition stress. Positive cold work is produced along the direct path and negative cold work is generated along the reverse path, which makes the cyclic transformation structurally reversible. At the same time, the transformation remains a nonequilibrium process in the sense that during both the direct and the reverse transitions energy is dissipated. Comparison of this behavior with the experimental results for a cubic-monoclinic transition in Ni–Ti shape memory wires under cyclic loading demonstrates good qualitative agreement. As we showed, it is also instructive to view the present model as a modification of the Preisach model with potentially richer response and with wider applications for different hysteretic systems.

There exist several directions along which our elementary model can be augmented. Thus one can consider an inhomogeneous chain with the elements differing in their

stiffnesses and the size of their spinodal regions (case of varying coercivities). One can show that such an inhomogeneous chain exhibits much more complex history dependence comparing to the case of identical springs; moreover, the chain with randomly distributed properties generates nonconstant heat/cold work ratio which is compatible with some recent experiments on metal plasticity. The application of the inhomogeneous model in the case of a hard device produces a realistic saw-tooth hysteresis with a characteristic hardening.

The extensions of the snap-spring model to the case of more than one dimension, further than nearest neighbor interaction, and several energy wells also presents an interesting challenge. The most nontrivial problems, however, are associated with the construction of the adequate continuum limit. As we showed the energy along our “optimal” path is a wiggly function of the total strain with the barriers inversely proportional to N . As the number of springs increases the potential energy (weakly) converges to the convex envelope of the corresponding function for a single spring. One can notice, however, that the derivatives of the energy exhibit rapid oscillations of finite amplitude which persist in the limit $N \rightarrow \infty$; as a result, the stress–strain relation for a discrete system cannot be obtained by differentiation of the limiting energy. The presence of a dense set of metastable configurations on the stress–strain diagram for a limiting system makes conventional purely elastic continuum limits at least questionable.

Acknowledgements

This work was supported by the research project Cofin-MURST2000 “Mathematical Models for Material Science” (GP) and by the NSF grant DMS-9803572 (LT).

References

- Abeyaratne, R., Chu, C., James, R.D., 1996. Kinetics of materials with wiggly energies: theory and applications to the evolution of twinning microstructures in a Cu–Al–Ni shape memory alloy. *Philos. Mag. A* 73 (2), 457–497.
- Achenbach, M., Müller, I., 1985. Shape memory as a thermally activated process. In: Sawczuk, A., Bandir, G. (Eds.), *Plasticity Today, Modeling, Methods and Applications*. Elsevier, London, New York.
- Allinger, T.L., Epstein, M., Herzog, W., 1996. Stability of muscle fibers on the descending limb of the force-length relation. A theoretical consideration. *J. Biomech.* 29 (5), 627–633.
- Balk, A.M., Cherkaev, A.V., Slepyan, L.I., 2001a. Dynamics of solids with non-monotone stress–strain relations. 1. Gibbs principle. *J. Mech. Phys. Sol.* 49, 131–148.
- Balk, A.M., Cherkaev, A.V., Slepyan, L.I., 2001b. Dynamics of solids with non-monotone stress–strain relations. 2. Nonlinear waves and waves of phase transition. *J. Mech. Phys. Sol.* 49, 149–171.
- Bertotti, G., 1999. *Hysteresis in Magnetism*. Academic Press, New York.
- Braides, A., Dal Maso, G., Garroni, A., 1999. Variational formulation of softening phenomena in Fracture Mechanics: the one-dimensional case. *Arch. Ration. Mech. Anal.* 146, 23–58.
- Collins, C., Luskin, M., 1994. Numerical modeling of the microstructure of crystals with symmetry related variants. In: Amad, L., Aizawa, M., Crowson, A., Rogers, C. (Eds.), *Technomic Publishing Company*. Lancaster, PA.
- Del Piero, G., Truskinovsky, L., 2000. Macro and micro cracking in 1D elasticity. *Int. J. Solids Struct.* 38, 1135–1148.
- Ericksen, J.L., 1975. Equilibrium of bars. *J. Elasticity* 5, 191–201.

- Fedelich, B., Zanzotto, G., 1992. Hysteresis in discrete systems of possibly interacting elements with a double-well energy. *J. Nonlinear Sci.* 2, 319–342.
- Huo, Y.Z., Müller, I., 1993. Nonequilibrium Thermodynamics of pseudoelasticity. *Cont. Mech. Therm.* 5, 163–204.
- James, R.D., 1996. Hysteresis in phase transformations. In: Kirchgassner, K., Mahrenholtz, O., Mennicken R., (Eds.), *Proceeding of the ICIAM95, Mathematical Research, Vol. 87*, Akademie Verlag, Berlin.
- James, R.D., Hane, K., 2000. Martensitic transformation and shape memory materials. *Acta Mater.* 48, 197–222.
- James, R.D., Wuttig, M., 1998. Magnetostriction of martensite. *Philos. Mag. A* 77, 1273–1299.
- Kinderlehrer, D., Ma, L., 1994. The simulation of hysteresis in nonlinear systems. In: Banks, H.T. (Ed.), *SPIE Smart Structures and Materials*, V. 2192, 78–87.
- Leo, P.H., Shield, T.W., Bruno, O.P., 1993. Transient heat transfer effects on the pseudoelastic behavior of shape memory wires. *Acta Metallar.* 41, 2477–2485.
- Macki, J.W., Nistri, P., Zecca, P., 1993. Mathematical models for hysteresis. *SIAM Rev.* 35 (1), 94–123.
- Maher, V.M., Crone, W.C., Shield, T.W., 1999. Displacement history effect on the pseudoelastic behavior of Shape-Memory wires. Preprint.
- Mayergoyz, I.D., 1991. *Mathematical Models of Hysteresis*. Springer, New York.
- Müller, I., 1979. A Model for a body with Shape-Memory. *Arch. Ration Mech. Anal.* 70, 61–77.
- Müller, I., Seelecke, S., 1996. Thermodynamics aspects of shape memory alloys. Reports of the Technical University of Berlin, Berlin.
- Müller, I., Villaggio, P., 1977. A model for an elastoplastic body. *Arch. Ration Mech. Anal.* 65, 25–46.
- Müller, I., Wilmansky, K., 1981. Memory alloys, phenomenology and Ersatz model. In: Brulin, O., Hsie, R.K.T. (Eds.), *Continuum Models of Discrete Systems, Vol. 4*. North-Holland, Pub. Co., Amsterdam.
- Ngan, S., Truskinovsky, L., 1999. Thermal trapping and kinetics of martensitic phase boundaries. *J. Mech. Phys. Solids* 47, 141–172.
- Ortin, J., 1992. Preisach modeling of hysteresis for a pseudoelastic Cu–Zn–Al single crystal. *J. Appl. Phys.* 71 (3), 1454–1461.
- Pagano, S., Paroni, R., 2000. A simple model for phase transitions: from the discrete to the continuum problem. Preprint.
- Puglisi, G., Truskinovsky, L., 2000. Mechanics of a discrete chain with bi-stable elements. *J. Mech. Phys. Solids* 1, 1–27.
- Ren, X., Truskinovsky, L., 2000. Finite scale microstructures in nonlocal elasticity. *J. Elasticity* 59, 319–355.
- Rogers, R., Truskinovsky, L., 1997. Discretization and hysteresis. *Physica B* 233 (4), 370–375.
- Rosakis, P., Rosakis, A.J., Ravichandran, G., Hodowany, J., 2000. A thermodynamic internal variable model for the partition of the plastic work into heat and stored energy in metals. *J. Mech. Phys. Solids* 48 (3), 581–607.
- Shaw, J.A., Kiriakides, S., 1995. Thermomechanical aspects of Ni–Ti. *J. Mech. Phys. Solids* 43, 1243–1281.
- Shield, T.W.P., Leo, H., Grebner, W.C.C., 1997. Quasi-static extension of Shape Memory wires under constant load. *Acta Mater.* 45, 67–74.
- Slepyan, L.I., 2000. Dynamic factor in impact, phase transition and fracture. *J. Mech. Phys. Solids* 48, 927–960.
- Slepyan, L.I., 2001. Feeding and dissipative waves in fracture and phase transition. II Phase transition waves. *J. Mech. Phys. Sol.* 49, 513–550.
- Slepyan, L.I., Troiankina, L.V., 1984. Fracture Wave in a Chain Structure. *J. Appl. Mech. Tech. Phys.* 25, 921–927.
- Struwe, M., 1990. *Variational Methods*. Springer, Berlin, Heidelberg.
- Truskinovsky, L., 1996. Fracture as phase transformation. In: Batra, R.C., Betty, M.F. (Eds.), *Contemporary Research in the Mechanics and Mathematics of Materials*. CIMNE, Barcelona, pp. 322–332.
- Truskinovsky, L., Zanzotto, G., 1996. Ericksen bar revisited: energy wiggles. *J. Mech. Phys. Solids* 44, 1371–1408.